Double quantum dot as a spin rotator

Konstantin Kikoin and Yshai Avishai
Ilse Katz Center for Nanotechnology and Department of Physics, Ben-Gurion University of the Negev, Beer Sheva 84105, Beer-Sheva, Israel

(Received 23 July 2001; published 8 March 2002)

It is shown that the low-energy spin states of double quantum dots (DQD's) with an even electron occupation number N possess a symmetry SO(4) similar to that of a rigid rotator familiar in quantum mechanics (rotational spectra of H_2 molecule, electron in Coulomb field, etc). The ''hidden symmetry'' of the rotator manifests itself in the tunneling properties of the DQD's. In particular, Kondo resonance may arise under an asymmetric gate voltage in spite of the even-electron occupation of the DQD. Various symmetry properties of a spin rotator in the context of the Kondo effect are discussed, and an experimental realization of this unusual scenario is proposed.

DOI: 10.1103/PhysRevB.65.115329 PACS number(s): 73.21.La, 72.10.−d

I. INTRODUCTION

In recent years, the physics of single-electron tunneling through a quantum dot (QD) under conditions of strong Coulomb blockades has been at the focus of intense investigation.[1] The number of electrons N in a dot can be regulated by a suitable gate voltage V_g applied to an electrode coupled capacitively to a dot. The Coulomb blockade suppresses the tunneling through the dot unless the resonance between its energies filled by N and $N+1$ electrons occurs at certain values of V_g, when it compensates for the charging energy, i.e., $\mathcal{E}(N+1,V_g)\approx\mathcal{E}(N,V_g)$. The differential conductance dI/dV_{sd} of a QD forms diamondlike patterns in the plan (V_{sd},V_g) where the nonconducting ''windows'' are separated by a network of Coulomb resonance lines (here V_{sd} is the source-drain voltage).

Accurate low-temperature experiments demonstrated the existence of Kondo resonances in windows corresponding to *odd* occupations of the dot[2] (O diamonds). These resonances are seen as zero-bias anomalies (ZBA's), i.e., as bridges of finite conductance connecting two opposite vertices of an O-diamond-shape window at $V_{sd}\to 0$. In addition, it was predicted theoretically[3] and observed experimentally[4] that Kondo resonances can also appear in even occupation windows (E diamonds) at strong enough magnetic fields. This unconventional magnetic-field-induced Kondo effect arises because the spectrum of the dot possesses a low-lying triplet excitation when the electron at the highest occupied level is excited with a spin-flip. The Zeeman energy compensates for the energy spacing between the two adjacent levels, and the lowest spin excitation possesses an effective spin 1/2, thus inducing a Kondo-like ZBA in the differential conductance.

A similar effect is possible in vertical quantum dots, for which the singlet and triplet states may be close in energy both at even and odd occupations. The influence of an external magnetic field on the orbital part of the wave functions of electrons in vertical quantum dots is, in general, more pronounced than the Zeeman effect. Hence singlet-triplet level crossings are induced by this field, causing the emergence of Kondo scattering at even filling or its enhancement at odd filling.[5] The theory of Kondo tunneling through vertical quantum dots in an external magnetic field was developed in Refs. 6–8.

In the present paper we explore yet another device which manifests the Kondo effect in QD's with an even electron number N, namely, a QD with two wells, which is referred to as a double quantum dot (DQD). A systematic treatment of the physics of DQD's with even N coupled to metallic leads is presented below. Special attention is given to the symmetry properties of a DQD, and its representation as a quantum spin rotator. It is well known[9] that the tunneling Hamiltonian for a QD can be mapped on the Kondo Hamiltonian in the O-diamond window of the QD. In the E-diamond window, the same procedure of eliminating the charged virtual states results in a four-state Hamiltonian of a doubly occupied dot where the singlet $S=0$ and triplet $S=1$ levels are intermixed by second-order tunneling. The coupling to a reservoir breaks the spin conservation in the quantum dot, and in the extended spin space formed by a singlet and triplet state the DQD acquires the dynamical symmetry SO(4) of a spin rotator, as shown in Ref. 10. As a Kondo scatterer, a spin rotator possesses interesting properties in comparison with localized spins obeying SU(2) symmetry. The magnetic-field-induced Kondo effect mentioned above is a manifestation of a ''hidden symmetry'' which is a footprint of the SO(4) group.

In Ref. 10 a special case was considered, namely, an asymmetric DQD formed by two dots of different radii in a parallel geometry coupled by a tunneling interaction with an even occupation $N=\nu_l+\nu_r$ (l and r stand for left and right, respectively). Moreover, it was assumed that a strong Coulomb blockade exists in one dot, whereas a tunneling contact with metallic leads exists in the other dot. Here we will address more general situations, and compare several representations in terms of effective spin Hamiltonians. It will be shown that unusual ZBA's can arise in generic DQD structures. In particular, a Kondo effect induced by quantum dots with SO(4) spin rotational properties also exists in an asymmetric DQD when both the l and r dots are coupled with the leads and the Coulomb blockade is strong enough in both of them. The main precondition for the emergence of a Kondo effect in this case is the sizable difference in ionization energies of the two dots. This quantity can, in fact, be tuned by

an application of a suitable gate voltage to one of them. The same effect can also be achieved in a symmetric DQD with even occupation in a parallel geometry, provided the axial symmetry of the system is broken by the difference in gate voltages applied to the right and left dots ($V_g^{r,l}$, respectively).

DQD's oriented parallel to the lead surfaces were fabricated several years ago.[11,12] Two main resonance effects were noted in such electric circuits. First, one of the dots (say, the right) can be used as an electrometer.[12] Scanning V_g^r at a fixed V_g^l, Coulomb oscillations can be induced both in the right and left dots because the interdot capacitive coupling changes the positions of the Coulomb resonance in both of them. As a result, the step wise structure of the conductance acquires a more complicated form. The Coulomb blockade windows between the resonances in the Coulomb energy of the dot $\mathcal{E}_{\nu_r,\nu_l}(V_g^r,V_g^l)$ form an ''egg-carton'' pattern,[11] where the vertices connect the windows with charge configurations (ν_r,ν_l), (ν_r,ν_l-1), and (ν_r+1,ν_l-1). The lines $\mathcal{E}_{\nu_l,\nu_r}\approx\mathcal{E}_{\nu_l+1,\nu_r}$, are the regions where the Coulomb resonance induced by V_g^r allows tunneling through the left dot. Second, the resonance $\mathcal{E}_{\nu_r,\nu_l}\approx\mathcal{E}_{\nu_r+1,\nu_l-1}$ allows cotunneling through the right and left dots, which is a precondition for the Kondo effect due to the appearance of a pseudospinlike configuration of the DQD.[13] Then, manipulating with V_g^r, one can induce a third transition $\nu_l-1,\nu_r+1\rightarrow\nu_l,\nu_r$ thus closing the loop and organizing the ''electron pump'' which transfers a single electron from one dot to another (see Ref. 14, and references therein).

The picture becomes even richer if the tunneling between the right and left wells of the DQD is taken into account. Then the dot can be treated an artificial molecule, where the interdot tunneling results in the formation of a complicated manifold of bonding and antibonding states[15] which modifies its charge degrees of freedom. In addition, it induces an indirect exchange, thus modifying the Kondo resonances when the dots are placed in series.[16] It will be shown below that the interdot tunneling in *parallel* geometry results in the appearance of a Kondo precursor of the Coulomb resonance along the lines $\mathcal{E}_{\nu_r,\nu_l}\approx\mathcal{E}_{\nu_r+1,\nu_l-1}$, $\mathcal{E}_{\nu_r,\nu_l}\approx\mathcal{E}_{\nu_r+1,\nu_l}$, and $\mathcal{E}_{\nu_r,\nu_l}\approx\mathcal{E}_{\nu_r,\nu_l+1}$ provided there exists a direct tunneling coupling V between the left and right dots. We consider the simplest case of $\nu_l=\nu_r=1$ in a neutral ground state of DQD's. It will be shown that an unconventional Kondo resonance occurs under the condition $V/[\mathcal{E}_{0,2}-\mathcal{E}_{1,1}]\ll 1$. Moreover, this kind of Kondo resonance can also appear in the middle of the Coulomb window for the right dot, provided the capacitance of the left dot essentially exceeds that of the right dot.[17] In both cases, the DQD possesses the symmetry of a spin rotator.

In Sec. II the various setups of DQD's are introduced, and the Hamiltonian describing the DQD is written down within the framework of a generalized Anderson model. The phase diagram of charging states in the left and right gate voltage plans is schematically drawn, and the regions of Kondo resonance are indicated. In the first part of Sec. III the spectrum of an isolated dot with even occupation is discussed. Section III B is devoted to the derivation and solution of renormalization-group equations for the DQD. The central result of this subsection is a demonstration of a possible singlet-triplet level crossing due to tunneling. When the renormalized energies are below the reduced band edge, renormalization stops, and charge fluctuations are suppressed. This is the Schrieffer-Wolff regime, and a derivation of an effective-spin Hamiltonian is executed in Sec. IV. In Sec. IV A, the spin Hamiltonian is given in terms of two vector operators and is shown to have the SO(4) symmetry of a spin rotator. This is followed by Sec. IV B, in which the renormalization-group flow of coupling constants is explained and the Kondo temperature is derived. Then, in Sec. IV C, a two-spin representation is suggested, in which the occurrence of two spin-1/2 operators just reflects the fact that the algebra o_4 is a direct sum of two o_3 algebras. In Sec. IV D, the possibility of arriving at the Kondo effect in a finite magnetic field is discussed, leading to a third representation of the spin Hamiltonian. The question of whether a DQD with two electrons can be regarded as a real two-site Kondo system (even if the DQD is highly asymmetric) is discussed in Sec. V. In particular, a stringent comparison is made with the two-spin representation mentioned in Sec. IV. The paper is concluded in Sec. VI. Some technical details of various calculations are relegated to the Appendix.

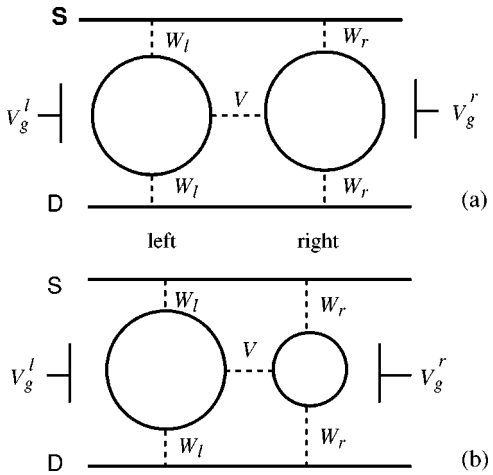

FIG. 1. Double quantum dots in parallel geometry. Left (l) and right (r) dots are coupled by tunneling V to each other and by tunneling $W_{l,r}$ to the source (S) and drain (D) electrodes. $V_g^{l,r}$ are the gate voltages. (a) Symmetric dot. (b) Asymmetric dot.

II. MODELS OF DOUBLE QUANTUM DOTS WITH SINGLET GROUND STATE

Two models considered in this work are sketched in Fig. 1. We will refer to a system (a) with zero gate voltages as a ''symmetric'' DQD. The same system with finite but unequal gate voltages $V_g^{l,r}$ will be called a ''biased'' DQD, and the pair of dots with different radii shown in Fig. 1(b) will be referred to as an ''asymmetric'' DQD.

In all cases the DQD is described by a generalized Anderson tunneling Hamiltonian which takes into account the internal structure of the DQD:

$$H=H_b+H_t+H_d+H_g. \tag{1}$$

The first term H_b is related to the lead electrons. They are described by Fermi operators $c_{k\sigma\alpha}$, where k is the quasimomentum, $\sigma=\pm 1/2$ is the spin projection, and $\alpha=s$ and d for source and drain electrodes. The corresponding energy dispersion is $\varepsilon_{k\alpha}$, so that

$$H_b=\sum_{k\sigma\alpha}\varepsilon_{k\alpha}c^{\dagger}_{k\sigma\alpha}c_{k\sigma\alpha}. \tag{2}$$

The second term H_t is the tunneling Hamiltonian, describing the hopping of dot electrons (described by Fermi operators $d_{i\sigma}$ with $i=l$ and r for left and right wells) into the leads, and vice versa. The corresponding tunneling amplitudes are $W_{k\alpha i}$. In fact, the lead dependence (subscript α) can be avoided using the transformation $c_{k\sigma}=2^{-1/2}(c_{k\sigma,s}+c_{k\sigma,d})$, and $W_{ki}=W_{k\alpha,i}/(W^2_{ks,i}+W^2_{kd,i})^{1/2}$. Thus

$$H_t=\sum_{i=l,r}\sum_{k\sigma}(W_{ki}c^{\dagger}_{k\sigma}d_{i\sigma}+\text{H.c.}). \tag{3}$$

The third term H_d describes an isolated DQD. In the present context, the quantum dot is a ''molecule,'' containing $N=\nu_{l0}+\nu_{r0}$ electrons in a neutral ground state. The geometry of the DQD prompts a two-channel approximation for the tunneling Hamiltonian. Indeed, in a symmetric DQD at $V_l=V_r$ the problem may be mapped onto a two-site spin scattering problem,[20] which, in turn is equivalent to a two-channel Kondo problem (see Sec. V for further details). However, our main concern is the asymmetric regimes where $V^l_g\neq V^r_g$ and/or the dots have essentially different radii. In these cases, as shown below, one of two channels (say, r) becomes irrelevant. The corresponding dot plays the part of a gate controlling the conditions for the charge and spin resonance tunneling through another dot (say, l). Therefore, one can assume a single channel from the very beginning without a loss of generality. Situations where the two-channel tunneling becomes crucially important are discussed in Ref. 8. The capacitive interaction *between the two wells of the* DQD is assumed to be strong enough to suppress the fluctuations of electron-tunneling-induced occupation in the windows between the Coulomb resonances of tunneling amplitude. We consider DQD's with even N, so that, generically, the ground state of an isolated DQD is a spin singlet. The isolated dot is then described by the Hamiltonian

$$H_d=\sum_{i=l,r}\sum_{\sigma}\epsilon_i n_{i\sigma}+V\sum_{i\neq j}d^{\dagger}_{i\sigma}d_{j\sigma}+H_{corr}, \tag{4}$$

in which V is the interwell constant tunneling amplitude. The capacitive interaction within the DQD is described by the term

$$H_{corr}=\frac{1}{2}\sum_i Q_i n_i(n_i-1)+Q_{lr}\delta n_l\delta n_r. \tag{5}$$

Here $n_i=\Sigma_\sigma d^{\dagger}_{i\sigma}d_{i\sigma}$, and $\delta n_i=n_i-\nu_{i0}$ is the deviation of the electron distribution from the neutral charge configuration ν_{i0} for a given DQD. Moreover, $Q_i=e^2/2C_i$ is the charging energy of a dot i whose capacitance is C_i, and Q_{lr} is the capacitive coupling between the left and right dots. The simplest configuration which contains, in a nutshell, all the complicated physics of many-body interactions arising in a course of tunneling is $N=2$, $\nu_{l0}=\nu_{r0}=1$. This case, for which $\delta n_i=n_i-1$, will be given special attention below. Finally, the term H_g represents the gate voltage energy. We consider symmetric and asymmetric DQD's formed by wells of equal and different radii, respectively (Fig. 1). Hence, generically, the gate potential H_g is asymmetric:

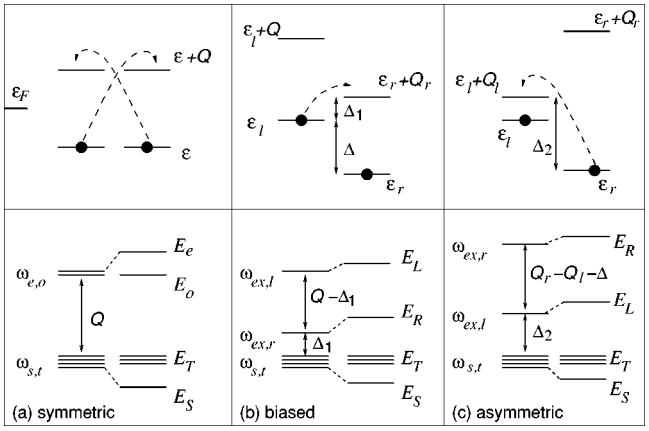

FIG. 2. Energy-level scheme for symmetric (a), biased (b) and asymmetric (c) DQD's. Upper panel: filled and empty one-electron levels. Dashed arrows indicate charge-transfer excitons. Lower panel: two-electron states of isolated and coupled left and right dots.

$$H_g=\sum_i V^i_g n_i, \quad V^l_g\neq V^r_g. \tag{6}$$

It is, in fact, useful to include the gate potential [Eq. (6)] in the position of the one-electron energy levels, $\varepsilon_i=\epsilon_i+V^i_g$. Then, by tuning the gate voltage, one can change the energy difference $\Delta=\varepsilon_l-\varepsilon_r$ or, in other words, redistribute the electron density between the left and right wells of the DQD.

It is assumed that in equilibrium and at zero gate voltages, each dot is filled by one electron and the Fermi level of the leads is in the middle of the Coulomb blockade window. The energy levels of a symmetric DQD with uncoupled dots ($Q_l=Q_r=Q$, $V=0$) are shown in the upper panel (a) of Fig. 2. These levels may be shifted relative to each other and to the Fermi level ε_F, and each level crossing $\varepsilon_i-\varepsilon_F$ corresponds to a recharging of the dot i. If electron exchange between the right dot and the leads is blocked,[11] the charge-transfer resonance between states $\{1,1\}$ and $\{0,2\}$ occurs when $\varepsilon_l=\varepsilon_r+Q$ (also see Ref. 18). In the general case [Fig. 1(a)], an additional electron appears in the dot i when the levels ε_i+Q and ε_F cross.

In the absence of interdot tunneling, $V=0$, one can easily obtain the effective spin Hamiltonian for a DQD with $N=2$ in a ground state far deep in the Coulomb blockade windows. For a symmetric DQD, this is a two-site Kondo Hamiltonian in window $\{1,1\}$ and two single-site Kondo Hamiltonians in windows $\{2,1\}$ and $\{1,2\}$. In the latter case of a charged DQD occupied by an odd number of electrons, tunneling through the left (right) dot is blocked, but a Kondo-type resonance compensates for the Coulomb block-

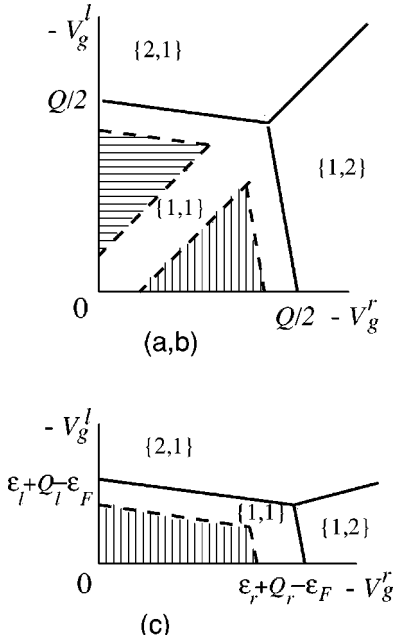

FIG. 3. Coulomb windows for different charge states $\{\nu_l,\nu_r\}$ of symmetric (a) and (b) and asymmetric (c) DQD's. Hatched regions indicate the domains where the Kondo effect exists.

ade and opens a tunneling channel through the right (left) dot. In the former case of a neutral DQD with even occupation, the possibility of Kondo tunneling is determined by the relative strength of the on-site indirect exchange J_i between spins S_i of singly occupied dots and conduction electrons in the reservoir, on the one hand, and the sign and magnitude of the intersite RKKY exchange J_{lr} on the other hand.[19] Both these parameters are predetermined by the tunnel coupling constants W_{ki} with the band electrons in the reservoir, but one can modify them by varying the gate voltages and interdot distance.

The interdot coupling modifies this picture significantly. It favors a singlet spin state in the middle of the Coulomb blockade window {1,1}, eliminating the Kondo tunneling at zero gate voltages. At finite $|V_g^l-V_g^r|$, the values of ν_i deviate from the integer values near the boundaries between the different charge sectors. Increasing negative gate voltages V_g^l or V_g^r, one can bias the charge distribution in favor of left or right dot, respectively, without changing the total number of electrons. As a result, with increasing $|V_g^l-V_g^r|$, one reaches a region of states with a small charge transfer gap $\Delta_1\equiv Q+\varepsilon_r-\varepsilon_l\ll Q$. The energy levels of such ''biased'' DQD's are shown in the upper panel of Fig. 2(b). These states occupy the upper right corner of the window {1,1} hatched in Fig. 3(a). Here the zero energy configuration illustrated by Fig. 2(a) corresponds to the coordinate origin. The virtual charge-transfer excitations [dashed arrow in the upper panel of Fig. 2(b)] significantly influence the tunneling through the DQD. It will be shown below that a type of Kondo resonance arises in this area of the sector {1,1}. The ''biased'' DQD in this sector behaves like a spin singlet at high temperatures and excitation energies, and demonstrates the properties of a spin-1 triplet partially screened by the Kondo tunneling at low energies and temperatures $T<T_K$. The Kondo temperature T_K is a function of $V_g^{l,r}$.

A similar effect exists for the asymmetric DQD [Fig. 1(c)], where the two coupled dots have different radii $r_l \gg r_r$ and hence different blockade energies $Q_l\ll Q_r$. The energy levels of an isolated DQD are shown in the upper panel of Fig. 2(c), and the corresponding recharging map is presented in Fig. 3(b). Here the hatched area also marks the region of the map where the Kondo effect arises in spite of the even number of electrons in the dot.

The question of whether to perceive the DQD with $N=2$ electrons as a two-center Kondo problem or as a generalized Anderson impurity is given special attention throughout this paper. A conventional approach for a description of the Kondo effect in a two-site quantum dot starts with a *two-center* Hamiltonian

$$H_{d0}=H_l+H_r, \tag{7}$$

and treats H_t in terms of a two channel tunneling operator

$$H_t=H_{tl}+H_{tr}. \tag{8}$$

The interdot interaction H_{lr} is considered as a coupling between two resonant Anderson centers. If the left and right dots each contain an odd number of electrons (as in our simplified model with $\nu_{l,r}=1$), Kondo tunneling is possible through each dot separately. The exchange part of the interdot coupling maps our Hamiltonian onto a two-site Kondo model. This coupling can be of both ferromagnetic and antiferromagnetic types. In the latter case the interplay between H_t and H_{lr} results in a suppression of Kondo tunneling through the left and/or right well of the DQD. The phase diagram of the two-site Kondo model was discussed in numerous papers.[19]

In the model discussed here, the interdot interaction is represented by the term $H_{lr}=V\Sigma_{i\neq j}d_{i\sigma}^{\dagger}d_{j\sigma}$, and we remain in the charge sectors {1,1}, {1,2}, and {2,1} of Fig. 3. It is obvious that this coupling suppresses Kondo tunneling through a symmetric DQD at zero gate voltages [point ''0'' in Fig. 3(a)], because the effective indirect exchange interaction which arises due to virtual excitations of charged states {0,2} and {2,0} is of antiferromagnetic sign, $J_{lr}=2V^2/Q$-like in the Heitler-London limit for a hydrogen molecule or in the half-filled Hubbard model. As a result, the ground state of a DQD is a spin singlet, and the gap $\delta=E_T-E_S=J_{lr}$, which divides the triplet excitation from the singlet spin ground state, prevents the formation of a Kondo resonance. It will be demonstrated below that this is not so in the case of *strongly asymmetric* DQD [hatched regions in Figs. 3(a) and 3(b)], where the crossover to a triplet state is induced by the tunneling H_t.

To describe this crossover, it is more convenient first to diagonalize the dot Hamiltonian H_d, i.e., to express it in the form

$$H_d=\sum_{N,\Lambda} E_{N\Lambda}|N\Lambda\rangle\langle N\Lambda|, \tag{9}$$

recalling that N is the number of electrons in a given charge state of the DQD, whereas Λ stands for a set of quantum numbers which characterize the many-electron configuration $d_l^{\nu_l} d_r^{\nu_r}$ in the presence of interdot coupling. In order to obtain a compact form for some equations, we introduce Hubbard projection and configuration change operators

$$X^{N\Lambda,N'\Lambda'} = |N\Lambda\rangle\langle N'\Lambda'|. \tag{10}$$

The diagonal terms $X^{N\Lambda,N\Lambda}$ are conventional projection operators, while the off-diagonal operators change the electron configuration of the dot. The tunneling term H_t [Eq. (3)] can now be rewritten in the form

$$H_t = \sum_{N,\Lambda} \sum_{N',\Lambda'} \sum_{k\sigma} (W_{k\sigma}^{N\Lambda,N'\Lambda'} X^{N\Lambda,N'\Lambda'} c_{k\sigma} + \text{H.c.}). \tag{11}$$

The matrix elements $W_{k\sigma}^{N\Lambda,N'\Lambda'}$ are nonzero for states in adjacent charge sectors of the eigenspace of H_d, so that $N = N' + 1$. In this approach, the DQD is treated as a "resonance impurity" in the framework of a conventional Anderson model, and its specific features are manifest in a characteristic energy spectrum $E_{N\Lambda}$ which includes contributions due to interdot tunneling and the Coulomb blockade.

III. DOUBLY OCCUPIED DQD AS AN ANDERSON IMPURITY

A. Energy levels and wave functions

Let us now employ the above approach for a doubly occupied DQD with $N=2$ in a charge sector $\{1,1\}$ of the Coulomb blockade diagram (Fig. 3). The dot Hamiltonian [Eqs. (4)–(6)] can be exactly diagonalized by using the basis of two-electron wave functions

$$|s\rangle = \frac{1}{\sqrt{2}} \sum_\sigma \sigma d_{l\sigma}^\dagger d_{r\bar{\sigma}}^\dagger |0\rangle,$$

$$|t_0\rangle = \frac{1}{\sqrt{2}} \sum_\sigma d_{l\sigma}^\dagger d_{r\bar{\sigma}}^\dagger |0\rangle, \quad |t_\sigma\rangle = d_{l\sigma}^\dagger d_{r\sigma}^\dagger |0\rangle, \tag{12}$$

$$|ex_l\rangle = d_{l\uparrow}^\dagger d_{l\downarrow}^\dagger |0\rangle, \quad |ex_r\rangle = d_{r\uparrow}^\dagger d_{r\downarrow}^\dagger |0\rangle.$$

Generically, the spectrum of a *neutral* DQD consists of a singlet ground state $|S\rangle$, a low-energy spin-1 triplet exciton $|T\mu\rangle$, and two high-energy charge-transfer singlet excitons $|Ex_l\rangle$ and $|Ex_r\rangle$. The corresponding two-electron wave functions are the following combinations:

$$|S\rangle = a_{ss}|s\rangle + a_{sl}|ex_l\rangle + a_{sr}|ex_r\rangle,$$

$$|T0\rangle = |t_0\rangle, \quad |T\pm\rangle = |t_\pm\rangle, \tag{13}$$

$$|Ex_l\rangle = a_{ll}|ex_l\rangle + a_{ls}|s\rangle, \quad |Ex_r\rangle = a_{rr}|ex_l\rangle + a_{rs}|s\rangle.$$

In the special case of symmetric DQD ($\varepsilon_l = \varepsilon_r$, $Q_l = Q_r$), the axial symmetry allows one to introduce even (e) and odd (o) excitonic states

$$|ex_{e,o}\rangle = \frac{1}{\sqrt{2}}(|ex_l\rangle \pm |ex_r\rangle).$$

The interdot tunneling leaves intact an odd singlet state $|ex_o\rangle$ as well as an odd triplet state $|T\mu\rangle$. As a result, one has, instead of Eq. (13),

$$|S\rangle = a_{ss}|s\rangle + a_{se}|ex_e\rangle, \quad |T\mu\rangle = |t_\mu\rangle,$$

$$|Ex_e\rangle = a_{ee}|ex_e\rangle + a_{es}|s\rangle, \quad |Ex_o\rangle = |ex_o\rangle \tag{14}$$

[see Fig. 2(a)]. We are mainly interested in the limiting cases of strongly biased symmetric DQD's where the interdot tunneling results in a sizable charge transfer between the left and right dots with a charge-transfer energy $\Delta_1 = \varepsilon_r + Q - \varepsilon_l$ [Fig. 2(b)], and an asymmetric dot with a charge-transfer energy $\Delta_2 = \varepsilon_l + Q_l - \varepsilon_r$ [Fig. 2(c)]. The virtual charge-transfer transitions which contribute to the lowest part of the energy spectrum are marked by dashed arrows. Charge fluctuations are negligible when

$$\beta = V/Q \ll 1, \quad \beta_1 = V/\Delta_1 \ll 1, \quad \beta_2 = V/\Delta_2 \ll 1, \tag{15}$$

in cases (a), (b), and (c) respectively.[20] The expansion coefficients a_{ij} in this limit are calculated for all three cases in the Appendix [Eqs. (A1), (A2), and (A3), also see the text and Ref. 21]. In a symmetric configuration (a) the two-electron levels which correspond to the bare states of a symmetric DQD form a low-energy quartet: $\omega_{s,t} = 2\varepsilon$ and $\omega_{ex_{e,o}} = 2\varepsilon + Q$. The odd states remain unrenormalized as a result of interdot tunneling, whereas the even states undergo a level repulsion. In the limit of small $\beta = V/Q \ll 1$,

$$E_S = 2\varepsilon - 2V\beta, \quad E_T = 2\varepsilon,$$

$$E_o = 2\varepsilon + Q, \quad E_e = 2\varepsilon + Q + 2V\beta, \tag{16}$$

[see the lower panel of Fig. 2(a)]. In the case (b) of a biased DQD, the two-electron bare energy levels are arranged as shown in the lower panel of Fig. 2(b):

$$\omega_{s,t} = \varepsilon_l + \varepsilon_r, \quad \omega_{ex,r} = \varepsilon_r + Q, \quad \omega_{ex,l} = \varepsilon_l + Q.$$

The parity is broken in this case, and the singlet state $|s\rangle$ is now hybridized with both excitonic states. In limit (15) one has

$$E_S = \varepsilon_l + \varepsilon_r - 2\beta_1 V, \quad E_T = \varepsilon_l + \varepsilon_r,$$

$$E_R = 2\varepsilon_r + Q + 2\beta_1 V, \quad E_L = 2\varepsilon_l + Q + 2\beta_1' V. \tag{17}$$

The role of the "left" exciton $|E_L\rangle$ in the low-energy processes is negligibly small. In the same spirit, all terms $\sim \beta_1' = V/(\varepsilon_l - \varepsilon_r + Q)$ will be neglected in pertinent calculations below.

The general scheme of energy eigenvalues in case (c) of an asymmetric DQD is similar to that of case (b), but here the first singlet excitation state is a charge-transfer exciton in the left dot. So the bare two-electron spectra are $\omega_{s,t} = \varepsilon_l + \varepsilon_r$, $\omega_{ex,l} = 2\varepsilon_l + Q_l$, $\omega_{ex,r} = 2\varepsilon_r + Q_r$, and the hybridized states are given approximately by

$$E_S=\varepsilon_l+\varepsilon_r-2\beta_2 V, \quad E_T=\varepsilon_l+\varepsilon_r,$$

$$E_L=2\varepsilon_l+Q_l+2\beta_2 V, \quad E_R=2\varepsilon_r+Q_r+2\beta_2' V \quad (18)$$

[see the lower panel of Fig. 2(c)]. In this case we neglect the contribution of "the right" exciton $|E_R\rangle$ and all terms $\sim\beta_2'=V/(\varepsilon_r-\varepsilon_l+Q_r)$.

It is seen from Eqs. (16), (17), and (18) for the energy spectrum of an isolated DQD that low-energy excitations with energy $\delta_s=E_T-E_S$ are dominantly of spin character, whereas the charge excitations $E_{e,o}$ in case (a) and $E_{L,R}$ in cases (b) and (c) are separated from the ground state by the gaps $\delta_{ch}\gg\delta_s$ in all three cases under consideration [lower panels of Figs. 2(a)–2(c)]. This same kind of "spin-charge separation" persists when the DQD is hybridized (via H_t) with itinerant electrons in the metallic reservoirs, on which we now focus our attention.

B. Renormalization of energy levels

The spectrum of electrons in the reservoirs is continuous, and forms a band with a bandwidth $2D_0$. In accordance with the renormalization-group (RG) procedure widely used in the conventional Anderson model, the low-energy physics can be exposed by integrating out the high-energy charge excitations in the framework of a "poor man's" scaling technique.[22] This procedure implies a renormalization of the energy levels and coupling constants of Hamiltonian (1) by mapping the initial energy spectrum $-D_0<\varepsilon<D_0$ onto a reduced energy band $-D_0+|\delta D|<\varepsilon<D_0-|\delta D|$.

The mapping procedure results in the following equations for the singlet and triplet renormalized energies of the DQD:

$$E_\Lambda\approx E_\Lambda^{(0)}+\sum_\lambda\sum_{q\sigma}\frac{|W_{q\sigma}^{\Lambda\lambda}|^2}{E_\Lambda-\epsilon_q-E_\lambda}, \quad (19)$$

where $E_\Lambda^{(0)}$ is the energy before renormalization, and $q=q_u$, and q_b are electron momenta such that ϵ_q belong to the layers $|\delta D|$ near the top or the bottom of the conduction band, respectively. They appear as intermediate virtual states in the processes of positive and negative ionizations of the DQD. The index $(\Lambda=S,T\mu)$ in these equations is reserved for the neutral two-electron states [Eq. (13)] of the DQD, whereas positively and negatively charged states with one and three electrons are designated by the index λ. The wave functions and energy levels of these states, as well as the matrix elements $W_{q,\sigma}^{\Lambda\lambda}$, are calculated in the Appendix. Figure 4 illustrates the processes involved in the level renormalization in all three cases under consideration. Note that these RG equations are uncoupled in this order. In accordance with the poor man's scaling approach,[22] only virtual transitions with an energy $\sim D$ are relevant, and the estimate of the sum on the right-hand side of Eq. (19) gives

$$E_\Lambda=E_\Lambda^{(0)}-\frac{\Gamma^\Lambda|\delta D|}{D}, \quad (20)$$

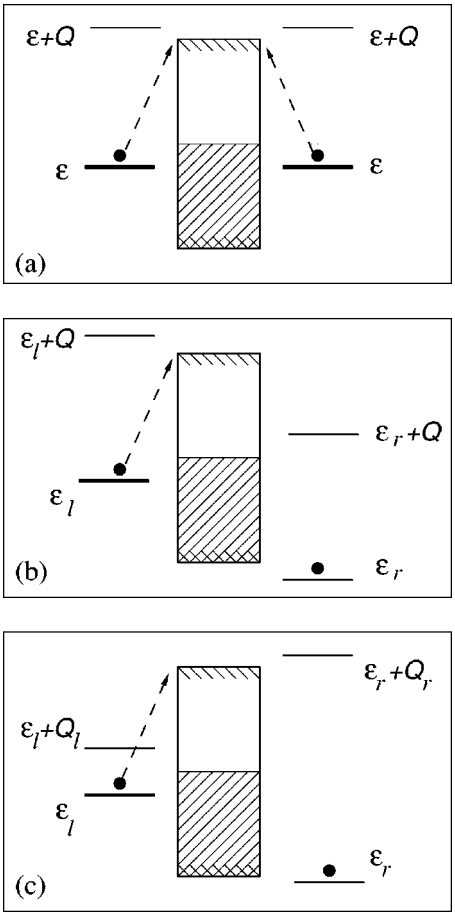

FIG. 4. The particle states, which are removed from a half-filled conduction band upon reducing the bandwidth by $|\delta D|$. The one-electron levels renormalized as a result of this process are shown by bold lines. (a) Symmetric DQD. (b) Biased DQD. (c) Asymmetric DQD.

where $\Gamma^\Lambda=\pi\rho_0|W^\Lambda|^2$, ρ_0 is the density of electron states in the reservoir, which is taken to be constant, and W^Λ are effective tunneling matrix elements calculated in the Appendix.

The crucial difference between the symmetric configuration (a) and the asymmetric configurations [(b) and (c)] is that the tunneling amplitudes of the processes involved in renormalization (19) are different for singlet and triplet states of the DQD. In the symmetric case (a), the left and right dot states are involved in renormalization of the two-electron states on an equal footing. The relevant processes are $|S\rangle\rightarrow|eq_u,1e\rangle$, $|S\rangle\rightarrow|oq_u,1o\rangle$, $T\rangle\rightarrow|oq_u,1e\rangle$, and $|T\rangle\rightarrow|eq_u,1o\rangle$. The one-electron tunneling transitions that make dominant contributions to these processes are shown by the dashed arrows in Fig. 4(a).

As a result, the tunneling rate in this case is

$$\Gamma_S=\Gamma_T\approx\pi\rho_0(|W_l|^2+|W_r|^2). \quad (21)$$

In the biased and asymmetric configurations (b) and (c) the even-odd symmetry is broken, and the Coulomb blockade in one center controls the tunneling through the other one.[11,12] Processes with energy $\sim D$ involve only electrons

from the left dot. The energy level ε_r is deep below the Fermi level, and renormalization (19) does not influence its position in accordance with the general argumentation of the scaling theory.[22] In case (b) the relevant processes are $|S\rangle \to |q_u\sigma, 1b\overline{\sigma}\rangle$, $|TO\rangle \to |q_u\sigma, 1b\overline{\sigma}\rangle$, $|T\pm\rangle \to |q_u\pm, 1_b\pm\rangle$, and the tunneling transitions which give the dominant contribution to these processes are shown by the dashed arrow in Fig. 4(b). The same kind of asymmetry takes place in case (c) [dashed arrows in Fig. 4(c)]. As a result, the right dot is excluded from the RG procedure, and one has, instead of Eq. (21),

$$\Gamma_T \approx \pi\rho_0 |W_l|^2, \quad \Gamma_S = a_{ss}^2 \Gamma_T. \tag{22}$$

Here the coefficient $a_{ss}<1$ is a measure of charge transfer from the left dot to the right dot due to admixture of singlet excitonic states to the ground state singlet [see Eqs. (A11) and (A12) in the Appendix]. Iterating the renormalization procedure [Eq. (20)], one comes to the pair of differential scaling equations

$$\frac{dE_\Lambda}{d\ln D} = \frac{\Gamma_\Lambda}{\pi}, \quad \Lambda = T,S, \tag{23}$$

which describes the evolution of the two-electron energy states when the energy scale of the band continuum is reduced. These equations describe not only the renormalization of the low-energy two-electron spin states, but also the change of the one-electron transition energies $E_\Lambda - E_\lambda$, because the one-electron states $\mathrm{E}_{\lambda=1b} = \varepsilon_r - O(\beta)$ are deep under the Fermi level, and the reduction of the energy scale does not influence them.

Scaling equations as in Eq. (23) were analyzed in Ref. 10 for a specific case of a ''Fulde molecule'' or double-shell quantum dot (DSD), where the electrons in one shell are subject to a strong correlation effect (Coulomb blockade) whereas the loosely bound electrons in the second shell are responsible for tunneling; also tunneling to the leads is allowed only for the second shell. Model (c) is a natural extension of a DSD because in the lowest approximation in the interdot interaction the tunneling through the right dot gives no contribution to level renormalization. In case (b), both left and right dots contribute to the renormalization procedure, but the crucial property of scaling equations, $\Gamma_S<\Gamma_T$ [see Eq. (22)] is shared by both configurations.

The scaling invariants for Eqs. (23) is

$$E_\Lambda^* = E_\Lambda(D) - \frac{\Gamma_\Lambda}{\pi}\ln\left(\frac{\pi D}{\Gamma_\Lambda}\right). \tag{24}$$

Here the scaling constants have to be chosen to satisfy the boundary condition $E_\Lambda(D_0) = E_\Lambda^{(0)}$. Due to relation (22) the energy $E_T(D)$ decreases with D faster than with $E_S(D)$, so that the two scaling trajectories E_Λ cross at a certain bandwidth $D = D_c$, estimated as

$$\frac{\Gamma_T - \Gamma_S}{\pi}\ln\frac{D_0}{D_c} = E_T^{(0)} - E_S^{(0)} \equiv \delta_0. \tag{25}$$

According to calculations performed in Ref. 10, this level crossing can occur either before or after the crossover to the Schrieffer-Wolff regime when the one-electron energies $E_\Lambda(D) - E_{1b}$ exceed the half-width of the reduced continuous spectrum $\overline{D} \sim |E_\Lambda(\overline{D}) - E_{1b}|$. In both cases, the charge degrees of freedom are quenched for excitation energies within the interval $-\overline{D} < \varepsilon < \overline{D}$, and a Haldane renormalization procedure should be replaced by the Anderson poor man's scaling.[23]

IV. SPIN HAMILTONIAN FOR DQD'S

A. Quantum rotator representation

The Schrieffer-Wolff transformation[24] for the configuration of two electron states of a DQD projects out those states of the dot having one electron or three electrons, and maps the Hamiltonian H onto an effective spin Hamiltonian $\tilde{H}$ acting in a subspace of two-electron configurations $\langle\Lambda| \ldots |\Lambda'\rangle$,

$$\tilde{H} = e^{\mathcal{S}} H e^{-\mathcal{S}} = H + \sum_m \frac{(-1)^m}{m!}\{\mathcal{S},[\mathcal{S}\ldots[\mathcal{S},H]]\ldots\}, \tag{26}$$

where

$$\mathcal{S} = \sum_{\Lambda\lambda}\sum_{\langle k\rangle\sigma} \frac{(W_\sigma^{\Lambda\lambda})^*}{\overline{E}_{\Lambda\lambda} - \epsilon_k} X^{\Lambda\lambda} c_{k\sigma} - \mathrm{H.c.} \tag{27}$$

Here $\langle k\rangle$ stands for the electron or hole states secluded within a layer $\pm\overline{D}$ around the Fermi level. $\overline{E}_{\Lambda\lambda} = E_\Lambda(\overline{D}) - E_\lambda(\overline{D})$. An effective Hamiltonian with the charged states $|\lambda\rangle = |1b\sigma\rangle, |3b\sigma\rangle$ frozen out can be obtained within first order in $\mathcal{S}$. As a result of integrating out the high-energy charge degrees of freedom, we are left with the effective spin Hamiltonian containing four states, $\Lambda = S,T$. The algebra of corresponding Hubbard operators is the o_4 algebra. Thus the DQD acquires an SO(4) symmetry, which is the dynamical symmetry of spin rotator. It has the form

$$\tilde{H} = \sum_\Lambda \overline{E}_\Lambda X^{\Lambda\Lambda} + \sum_{\langle k\rangle\sigma} \epsilon_k c_{k\sigma}^\dagger c_{k\sigma} - \sum_{\Lambda\Lambda'\lambda}\sum_{kk'\sigma\sigma'} J_{kk'}^{\Lambda\Lambda'\lambda} X^{\Lambda\Lambda'} c_{k\sigma}^\dagger c_{k'\sigma'}, \tag{28}$$

where

$$J_{kk'}^{\Lambda\Lambda'\lambda} = (W_\sigma^{\Lambda\lambda})^* W_{\sigma'}^{\Lambda'\lambda}\left(\frac{1}{\overline{E}_{\Lambda\lambda} - \epsilon_k} + \frac{1}{\overline{E}_{\Lambda'\lambda} - \epsilon_{k'}}\right).$$

In the charge sector $N=2$ the constraint $\Sigma_\Lambda X^{\Lambda\Lambda} = 1$ is valid. As shown in Refs. 7 and 10, the effective Schrieffer-Wolff Hamiltonian of DQD describes not only the conventional indirect exchange between localized and itinerant spins. It also contains terms that intermix the singlet and triplet states of the quantum dot. This mixing is due to the tunneling exchange with electrons in the metallic reservoir.

Before writing down the pertinent spin Hamiltonian, a few words about a quantum spin rotator are in order. It is known (see, e.g., Ref. 25) that the symmetry of a standard quantum rotator is described by an operator of rotational angular momentum **L** and an additional vector operator **M**. These two operators generate the semisimple algebra o_4; they are orthogonal, $\mathbf{L}\cdot\mathbf{M}=0$, and the corresponding Casimir operator is $\mathbf{L}^2+\mathbf{M}^2$. The matrix elements of the operator **M** connect states with different values of the orbital momentum $l\rightarrow l\pm 1$. The existence of this second operator reflects the ''hidden angular symmetry'' of the rotator.

Similarly, the spin symmetry of the DQD is characterized not only by the spin-1 vector **S**: one can introduce a second vector operator **P** orthogonal to **S** which determines the matrix elements of transitions between the different states of the rotation group SO(4). In the present case, the vector $\mathbf{P}=\{P_z,P^{\pm}\}$ determines the transitions between the singlet state and the different components of the spin triplet. It is convenient to express the spherical components of the vector operator **P** in terms of Hubbard operators $X^{\Lambda\Lambda'}$ (for brevity, $\Lambda\Lambda'$ will be either S for a singlet quantum number or $\mu=1$, 0, and $\bar{1}$ for triplet magnetic quantum numbers):

$$P^+=\sqrt{2}(X^{1S}-X^{S\bar{1}}),\quad P^-=\sqrt{2}(X^{S1}-X^{\bar{1}S}),$$

$$P_z=-(X^{0S}+X^{S0}). \tag{29}$$

Within the same procedure, the spherical components of the spin-1 operator **S** are given by the following expressions:

$$S^+=\sqrt{2}(X^{10}+X^{0\bar{1}}),$$

$$S^-=\sqrt{2}(X^{01}+X^{\bar{1}0}),\quad S_z=X^{11}-X^{\bar{1}\bar{1}}. \tag{30}$$

The vector operators **P** and **S** obey the commutation relations of the usual o_4 Lie algebra:

$$[S_j,S_k]=ie_{jkl}S_l,\quad [P_j,P_k]=ie_{jkl}S_l,\quad [P_j,S_k]=ie_{jkl}P_l \tag{31}$$

(here j,k,l are Cartesian indices). In addition, the following relations hold:

$$\mathbf{S}\cdot\mathbf{P}=0,\ S^2=2(1-X^{SS}),\ P^2=1+2X^{SS}. \tag{32}$$

To wit, **S** (a spin 1) and **P** are two orthogonal vector operators in spin space which generate the algebra o_4 in a representation specified by the Casimir operator $\mathbf{S}^2+\mathbf{P}^2=3$. This justifies the qualification of a DQD as a *spin rotator*.

Returning back to the effective spin Hamiltonian, Eq. (28) it now acquires a more symmetric form

$$\tilde{H}=\tilde{H}^S+\tilde{H}^T+\tilde{H}^{ST}, \tag{33}$$

where

$$\tilde{H}^S=\bar{E}_S X^{SS}+J^S\sum_{\sigma} X^{SS}n_{\sigma},$$

$$\tilde{H}^T=\bar{E}_T\sum_{\mu} X^{\mu\mu}+J^T\mathbf{S}\cdot\mathbf{s}+\frac{J_T}{2}\sum_{\mu\sigma} X^{\mu\mu}n_{\sigma}, \tag{34}$$

$$\tilde{H}^{ST}=J^{ST}(\mathbf{P}\cdot\mathbf{s}).$$

The local electron operators are defined as usual,

$$n_{\sigma}=c_{\sigma}^{\dagger}c_{\sigma}=\sum_{kk'} c_{k\sigma}^{\dagger}c_{k\sigma},\quad \mathbf{s}=2^{-1/2}\sum_{kk'}\sum_{\sigma\sigma'} c_{k\sigma}^{\dagger}\hat{\tau}c_{k'\sigma'}, \tag{35}$$

and $\hat{\tau}$ are the Pauli matrices. Moreover, the coupling constants are

$$J^T=\left(\frac{|W_l|^2}{\varepsilon_F-\epsilon_l}+\frac{|W_r|^2}{E_r+Q-\varepsilon_F}\right) \tag{36}$$

in case (b), and

$$J^T=|W_l|^2\left(\frac{1}{\varepsilon_F-\epsilon_l}+\frac{1}{E_l+Q_l-\varepsilon_F}\right) \tag{37}$$

in case (c). In both cases

$$J^S=a_{ss}^2J^T,\quad J^{ST}=a_{ss}J^T. \tag{38}$$

This completes the derivation of the spin rotator Hamiltonian for a DQD hybridized with itinerant electrons.

B. RG flow of coupling constants: Kondo temperature

Due to the intermixing term $\tilde{H}_{ST}$ in the spin Hamiltonian [Eq. (34)], both triplet and singlet states are involved in the formation of the low-energy spectrum of the DQD. Scaling equations for the coupling constants J^T and J^{ST} can be derived by the poor man's scaling method of Ref. 23. Neglecting the irrelevant potential scattering phase shift and using the above-mentioned procedure of integrating out the high-energy states, a pair of scaling equations is obtained:

$$\frac{dj_1}{d\ln d}=-[(j_1)^2+(j_2)^2],\quad \frac{dj_2}{d\ln d}=-2j_1j_2 \tag{39}$$

(here $j_1=\rho_0J^T$, $j_2=\rho_0J^{ST}$, and $d=\rho_0D$). If $\bar{\delta}=E_T(\bar{D})-E_S(\bar{D})$ is the smallest energy scale, the energy spectrum of the DQD is quasidegenerate, and system (39) is reduced to a single equation for the effective integral $j_+=j_1+j_2$;

$$\frac{dj_+}{d\ln d}=-(j_+)^2. \tag{40}$$

Then the RG flow diagram has an infinite fixed point, and the solution of Eq. (40) gives the Kondo temperature

$$T_{K0}=\bar{D}\exp(-1/j_+). \tag{41}$$

In the general case, the scaling behavior is more complicated. The flow diagram still has a fixed point at infinity, but the Kondo temperature turns out to be a sharp function of $\bar{\delta}$. In the case $\bar{\delta}<0$, $|\bar{\delta}|\gg T_{K0}$ considered in Refs. 7, 8, and 10 the scaling of J^{ST} terminates at $D\simeq\bar{\delta}$. Then one is left with the familiar physics of an underscreened $S=1$ Kondo model.[27] The fixed point is still at infinite exchange coupling

J_T, but the Kondo temperature becomes a function of $\overline{\delta}$. It was shown in Ref. 8 that a kind of universal law for $T_K(\overline{\delta})$ also exists in this limit,

$$T_K/T_{K0}=(T_{K0}/\overline{\delta})^{\gamma}, \tag{42}$$

where γ is a numerical constant. Now we can explain the diagram illustrating the appearance of the Kondo tunneling regime in a Coulomb window with even occupation $\{1,1\}$ (Fig. 3). In the case of symmetric H_2-like DQD (the upper panel of Fig. 1) the tunneling is predetermined by the parameters $\varepsilon\equiv\varepsilon_l=\varepsilon_r$, $W\equiv W_g^l=W_g^r$, Q, and V, and the difference $|V_g^l-V_g^r|$. If the parameters ε, W, Q, and V, characterizing the device, are fixed, then the tunneling regime is controlled by the external gate voltage $\Delta=|V_g^l-V_g^r|$ [see Fig. 2(b)]. This voltage enters the initial singlet-triplet energy gap $\delta_0=2V^2/(Q-\Delta)$ as well as the coefficient a_{ss}^2 characterizing the asymmetry of tunneling rates $\Gamma_{T,S}$ [see Eqs. (15), (22), (A1), and (A2)].

At $\Delta=0$ (zero voltage), the tunneling rates are equal, $\Gamma_T=\Gamma_S$, so the DQD remains in a singlet state in spite of tunneling renormalization, and the Kondo tunneling is absent along the diagonal of the $\{1,1\}$ window in the upper panel of Fig. 3. At small Δ the asymmetry is weak enough to satisfy criterion (25) for crossing of the scaling trajectories $E_{T,S}(D)$, so the stripe of zero conductance around the diagonal has a finite width. With increasing voltage Δ both δ_0 and $\Gamma_T-\Gamma_S$ grow together with growing $\beta_1=V/(Q-\Delta)$. However, the former difference is $\sim\beta_1$, while the latter one is $\sim\beta_1^2$ and grows more quickly. As a result, beginning from a certain Δ, criterion (25) is satisfied, and we enter the domain of Kondo tunneling (the hatched areas in the upper panel of Fig. 3). On the other hand, when Δ is too large, and the parameter $\beta_1>1$, one enters a region of strong charge fluctuations in the vicinity of the Coulomb resonance, and the Kondo effect should disappear as a result. The theoretical picture of interplay between spin and charge tunneling channels region in this region is still not clear. Since the behavior of the systems depends only on the modulus $|V_g^l-V_g^r|$, the diagram is symmetric around the diagonal of the Coulomb window.

Unlike the case of a H_2-like DQD, one may expect that the Kondo tunneling regime is realized at zero voltage in an asymmetric DQD (Fig. 1, lower panel). In terms of the above theory this means that criterion (25) is already satisfied at $V_g^l=V_g^r=0$. This situation was considered in Ref. 10. Then the role of the gate voltage is to drive the system toward the lines of Coulomb resonance, so we come to the picture schematically drawn in the lower panel of Fig. 3.

C. Two-spin representation

It is known[25] that the algebra o_4 can be represented as a direct sum of two o_3 algebras. In our case this means that one can construct another pair of orthogonal operators

$$\mathbf{S}_1=\frac{\mathbf{S}+\mathbf{P}}{2},\quad \mathbf{S}_2=\frac{\mathbf{S}-\mathbf{P}}{2} \tag{43}$$

(also see Ref. 8). In the Hubbard representation the components of these spin vectors have forms

$$\begin{aligned}
S_{1,2}^{+}&=\frac{1}{\sqrt{2}}(X^{10}+X^{0\bar{1}}\pm X^{1S}\mp X^{S\bar{1}}),\\
S_{1,2}^{-}&=\frac{1}{\sqrt{2}}(X^{01}+X^{\bar{1}0}\pm X^{S1}\mp X^{\bar{1}S}),\\
S_{z1,2}&=\frac{1}{2}(X^{1\bar{1}}+X^{\bar{1}\bar{1}}\mp X^{0S}\mp X^{S0}).
\end{aligned} \tag{44}$$

It is easy to check by direct substitution that

$$S_i^2=3/4,\ X^{SS}=\frac{1}{4}-(\mathbf{S}_1\cdot\mathbf{S}_2),\quad \sum_{\mu}X^{\mu\mu}=\frac{3}{4}+(\mathbf{S}_1\cdot\mathbf{S}_2). \tag{45}$$

The Casimir operator can be introduced as $4\mathbf{S}_1^2=4\mathbf{S}_2^2$.

Then substituting Eqs. (43) and (44) into Hamiltonian (33), we rewrite it in the form

$$\tilde{H}=J(\mathbf{S}_1\cdot\mathbf{S}_2)+J_1(\mathbf{S}_1\cdot\mathbf{s})+J_2(\mathbf{S}_2\cdot\mathbf{s})+J_3(\mathbf{S}_1\cdot\mathbf{S}_2)\sum_{\sigma}n_{\sigma}+\text{const}. \tag{46}$$

Here

$$J=\overline{E}_T-\overline{E}_S\equiv\overline{\delta},\quad J_{1,2}=J^T\pm J^{ST},\quad J_3=\frac{1}{2}J_T-J_S. \tag{47}$$

Thus, as mentioned in Ref. 8, transformation (43) maps Hamiltonian (33) on an effective two-spin Kondo Hamiltonian plus an additional potential scattering term. However, the physical meaning of these two spin operators differs from that in the conventional two-site Kondo model.[19] They only span the two o_3 subalgebras of the semisimple Lie algebra o_4 (see Sec. V for further discussion).

This kind of effective Hamiltonian also appears in other situations where singlet and triplet states of a nanoobject close in energy, e.g., in vertical quantum dots[6,7] or in conventional dots at even occupation, provided low-lying triplet excitons are taken into account.[3,8] It was noted in Refs. 7, 8, and 10 that the interplay between two energy scales, i.e., the interdot singlet-triplet gap δ and the tunneling-induced Kondo binding energy for a triplet configuration $\Delta_T\sim\overline{D}\exp(-1/\rho_0 J_T)$ results in an essentially nonuniversal behavior of the Kondo temperature T_K (see Sec. IV B).

D. Magnetic-field-induced Kondo effect

Yet another peculiar manifestation of the ''hidden symmetry'' of the spin rotator is the possible occurrence of a magnetic-field-induced Kondo effect. Such a possibility was discussed theoretically in Ref. 3 for the case of quantum dots formed in GaAs heterostructures, and in Refs. 8, 6, and 7 for the case of vertical quantum dots where the external magnetic field influences the orbital part of spatially quantized

wave functions and results in singlet-triplet level crossing. In DQD, similar effect arises if $\overline{\delta} > 0$, where the ground state of the DQD remains a singlet in spite of the tunneling-induced renormalization. Here we rederive the field-induced Kondo effect in terms of a spin rotator representation.

In an external magnetic field, the energy levels in $\tilde{H}^T$ are split due to the Zeeman effect, $\tilde{E}_T \to \tilde{E}_{T\mu} = \tilde{E}_T - \mu\delta_Z$. As noted in Ref. 3, the Zeeman splitting $\delta_Z = g\mu_B B$ of the excited triplet state compensates for the energy gap $\overline{\delta}$ at a certain value of magnetic field $B = B_0$. In the vicinity of this point when $\delta - \delta_Z \ll \delta$, only the levels $\tilde{E}_{T1}$ and $\tilde{E}_S$ survive in the diagonal part $\overline{E}_S X^{SS} + \overline{E}_T \Sigma_\mu X^{\mu\mu}$ of the spin rotator Hamiltonian [Eq. (34)]. Then the only renormalizable coupling parameter in the exchange Hamiltonian [Eq. (34)] is J^{ST}. It is easily seen that the operators P^+, P^-, and $(S_z - X^{SS})$ form an algebra o_3 in the reduced spin space $\{S, T1\}$. In this subspace the operators P^+ and P^- are reduced to $\sqrt{2}X^{1S}$ and $\sqrt{2}X^{S1}$, respectively. The operators $S^+ \to \sqrt{2}X^{0\overline{1}}$ and $S^- \to \sqrt{2}X^{\overline{1}0}$, together with a combination $(X^{00} - X^{\overline{1}\overline{1}})$, act in the subspace of excited states $\{T0, T\overline{1}\}$ divided by the Zeeman energy from the low-energy doublet. These operators form a complementary algebra o_3, and the direct sum of these algebras represent a realization of the SO(4) symmetry for a ''spin rotator in an external magnetic field'' when the rotational symmetry in spin space is broken.

As a result, the effective spin Hamiltonian [Eq. (34)] in a subspace $\{S, T1\}$ reduces to

$$\tilde{H}_Z = E_Z R_0 + J^{ST}(\mathbf{R}\cdot\mathbf{s}) + H_p. \tag{48}$$

Here $E_Z = \overline{E}_S = \overline{E}_{T1}$ is the degenerate ground-state energy level of a DQD in a magnetic field $B = B_0$, H_p describes irrelevant potential scattering, and the operators R_0, and $\mathbf{R}$ are

$$R_0 = X^{11} + X^{SS}, \quad R_z = X^{11} - X^{SS},$$
$$R^+ = \sqrt{2}X^{1S}, \quad R^- = \sqrt{2}X^{S1}. \tag{49}$$

The complementary vector $\mathbf{T}$, defined as

$$T_z = X^{00} - X^{\overline{1}\overline{1}}, \quad T^+ = \sqrt{2}X^{0\overline{1}}, \quad T^- = \sqrt{2}X^{\overline{1}0}, \tag{50}$$

forms a second subgroup. This vector is quenched by the magnetic field. The spectrum of conduction electrons is also split due to Zeeman effect, but this splitting does not affect the Kondo singularity in the tunnel current: one may simply redefine the conduction-electron energies and measure them from the corresponding Fermi levels for spin-up and -down electrons.[8]

Applying the poor man's scaling procedure[23] to Hamiltonian (48), one comes to a scaling equation

$$\frac{dj_2}{d\ln D} = -(j_2)^2, \tag{51}$$

with a fixed point at $j_2 = \infty$ and the Kondo temperature $T_{KZ} = \overline{D}\exp(-1/j_2)$, so that

$$\frac{T_K}{T_{K0}} = \exp\left(-\frac{1}{1+a_{ss}}\right). \tag{52}$$

Of course, the same kind of separation is possible for a degenerate pair of states $\tilde{E}_S$ and $\tilde{E}_{T\overline{1}}$, and the corresponding vectors $\mathbf{R}'$ and $\mathbf{T}'$ may be obtained from Eqs. (49) and (50) by interchanging indices 1 and $\overline{1}$ (see Ref. 8 for a physical realization of this situation).

To summarize the description of basic manifestations of spin rotator symmetry in DQD's, we considered three limiting cases of spin rotator representations depending on the physical situations: quasidegenerate state $|\overline{\delta}| \ll T_K$, when the resonance properties of a DQD are determined by the full SO(4) symmetry [Eq. (41)]; triplet ground state $|\overline{\delta}| > T_K$, where the virtual excitations to singlet state render the Kondo temperature dependent on the initial singlet/triplet splitting [Eq. (42)]; and a magnetic-field-induced doublet ground state [Eq. (51)], where the Kondo resonance arises in spite of the loss of local rotational invariance. The hierarchy of Kondo temperatures is nonuniversal. The maximal value of T_K is given by T_{K0} [Eq. (41)], from which it falls with the removal of singlet/triplet degeneracy.[7,8] It then reaches the limiting value of $\overline{D}\exp(-1/j_1)$ at large $\overline{\delta}$, where the contribution of the high-lying singlet state becomes negligibly weak, and one returns back to the typical SU(2) symmetry of spin $S = 1$ described by the o_3 algebra.

All the above results could also be obtained in representation (44). In this case the scaling equations should be derived for three coupling constants J_1, J_2, and J_3 of the spin Hamiltonian [Eq. (46)]. This procedure was described in Ref. 8. As expected, the results are equivalent since the scaling of J_3 adds nothing to the singular behavior of the relevant parameters J_T and J_{ST}. The problem becomes more complicated in case there are two sources and two drains.[13] Then an additional index α should be introduced for the lead electrons $c_{k\sigma} \to c_{\alpha k\sigma}$. States with different α's are intermixed due to interdot tunneling, and one more operator $\mathbf{S}\times\mathbf{P}$ or $\mathbf{S}_1\times\mathbf{S}_2$ should be introduced in the theory of a spin rotator coupled to metallic leads.[8]

V. TWO-CENTER KONDO MODEL FOR DQD'S

It is natural to expect that in the limit of vanishing interdot coupling V the tunneling through a doubly occupied DQD is defined by the individual spins $S = 1/2$ of the left and right dots, and the existence or nonexistence of a resonance tunneling channel will be predetermined by the competition between the Kondo effect for the left and right dots and the indirect exchange induced by the same tunneling. In this limit the problem is reduced to a specific version of the two-site Kondo model. The corresponding theory for a *symmetric* two-site Kondo impurity in a metal was discussed, e.g., in Ref. 19. The question is how this approach should be modified in the asymmetric cases (b) and (c). On the other hand, with increasing V, these two approaches should be matched, and it is instructive to compare the description of a DQD by two fictitious spins [Eqs. (43)] and by two real spins $\mathbf{S}_l$ and $\mathbf{S}_r$.

To study this problem we use the approach mentioned in Sec. II, and consider the DQD as a two-site center with spins 1/2 in each site within the framework specified by Hamiltonians (7) and (8). In terms of Hubbard operators (10) for spin 1/2, this Hamiltonian is written as $H=H_{do}+H_t+H_{lr}$, where

$$H_{do}=\sum_{i,\Lambda} E_{i\Lambda}X_i^{\Lambda\Lambda} \quad (\Lambda=0,\sigma,2),$$

$$H_t=\sum_{i,k\sigma}[W_{ik\sigma}(X_i^{\sigma 0}+X_i^{2\bar{\sigma}})c_{k\sigma}+\text{H.c.}]. \tag{53}$$

In case (b), the states E_{l0}, $E_{l\sigma}=\varepsilon_l$, $E_{r\sigma}=\varepsilon_r$, and $E_{r2}=2\varepsilon_r+Q$ are involved in the RG procedure, and the corresponding interdot tunneling Hamiltonian is represented in the form

$$H_{lr}=V\sum_{\sigma}(X_l^{\sigma 0}X_r^{\bar{\sigma}2}+\text{H.c.}). \tag{54}$$

This tunneling is possible only in the singlet configuration of the DQD. We start by eliminating the polar states $\{l0,r2\}$ that arise due to interdot tunneling [Eq. (54)]. This procedure, known as a Harris-Lange canonical transformation,[26] eliminates the interdot term H_{lr}, and instead, in second order in V, an interdot spin-Hamiltonian emerges,

$$H_{lrs}=J_{lr}\sum_{\sigma\sigma'}X_l^{\sigma\sigma'}X_r^{\sigma'\sigma}, \tag{55}$$

where $J_{lr}=V^2/\Delta_1$.

As in Sec. IV, we should integrate out the high-energy charged states by using the Haldane RG procedure[22] for the left dot alone, since the renormalization of the deep level ϵ_r is negligible. However this procedure should now include the renormalization of J_{lr} due to a reduction of the conduction band. The scaling equation for ε_l is the same as Eq. (24) for a triplet state. We rewrite it in terms of the two-spin Hamiltonian as

$$\frac{d\varepsilon_l}{d\ln D}=\frac{\Gamma_l}{\pi} \tag{56}$$

($\Gamma_l\equiv\Gamma_T$). The same mapping procedure as in Eq. (19) gives a correction to the indirect exchange coupling constant,

$$\tilde{J}_{lr}=J_{lr}-\frac{\beta_1^2\Gamma_l|\delta D}{D}, \tag{57}$$

and its iteration results in the second scaling equation;

$$\frac{dJ_{lr}}{d\ln D}=-\beta_1^2\frac{\Gamma_l}{\pi}. \tag{58}$$

This procedure stops at $D=\bar{D}$, where the Schrieffer-Wolff limit for ϵ_l is achieved. Integrating Eq. (58) from $\bar{D}$ to D_0, one comes to the following equation for the renormalized indirect exchange coupling:

$$J_{lr}(\bar{D})=J_{lr}(D_0)-\beta_1^2\Gamma_l\ln(D_0/\bar{D}).$$

Then, taking into account that $\delta=J_{lr}$ by its origin, this equation can be rewritten in the form

$$\bar{\delta}=\delta_0-\beta_1^2\Gamma_l\ln(D_0/\bar{D}). \tag{59}$$

This is the same result for the renormalized singlet-triplet excitation energy that we found in Sec. IV. In case (c), a similar procedure starts by eliminating the polar states generated by the interdot tunneling term [see Fig. 3(c)]:

$$H_{lr}=V\sum_{\sigma}[X_l^{2\bar{\sigma}}X_r^{0\sigma}+\text{H.c.}]. \tag{60}$$

In this case the Harris-Lange procedure results in an indirect exchange Hamiltonian [Eq. (55)], with a coupling constant $J_{lr}=V^2/\Delta_2$. Again, only the energy level ε_l is involved in Haldane's RG procedure. Scaling equation (58) contains, on the right-hand side, the factor β_2 instead of β_1, and its solution for the triplet/singlet level splitting gives

$$\bar{\delta}=\delta_0-\beta_2^2\Gamma_l\ln(D_0/\bar{D}). \tag{61}$$

This is exactly the result obtained in Ref. 10.

Next the Schrieffer-Wolff transformation eliminates the tunnel coupling. The operator $\mathcal{S}$ in Eq. (26) has the form

$$\mathcal{S}=\sum_{k\sigma}\frac{W_l}{\varepsilon_k-\varepsilon_l}(X_l^{\sigma 0}c_{k\sigma}^{\dagger}-\text{H.c.}) + \sum_{k\sigma}\frac{W_l}{\varepsilon_l+Q-\varepsilon_k}(X_l^{2\bar{\sigma}}c_{k\sigma}-\text{H.c.}), \tag{62}$$

in case (b), and

$$\mathcal{S}=\sum_{k\sigma}\frac{W_l}{\varepsilon_k-\varepsilon_l}(X_l^{\sigma 0}c_{k\sigma}^{\dagger}-\text{H.c.}) \tag{63}$$

in case (c). As usual, in second order, the tunneling term generates an indirect exchange between the leads and dots. As a result, the total spin Hamiltonian acquires the form

$$H_s=\bar{J}_{lr}(\mathbf{S}_l\cdot\mathbf{S}_r)+\sum_{i=l,r}J_i(\mathbf{S}_i\cdot\mathbf{s})+H'. \tag{64}$$

Here $\bar{J}_{lr}=\bar{\delta}$ is the renormalized singlet/triplet excitation energy [Eq. (59) or (61)] in cases (b) and (c), respectively. The components of the local spins $\mathbf{S}_i$ are now defined as

$$S_i^{+}=X_i^{\uparrow\downarrow}, \quad S_i^{-}=X_i^{\downarrow\uparrow}, \quad S_{iz}=\frac{1}{2}(X_i^{\uparrow\uparrow}-X_i^{\downarrow\downarrow}). \tag{65}$$

The Heisenberg-like interdot exchange [Eq. (64)] arose in second order in V similarly to the effective antiferromagnetic exchange in a half-filled Hubbard model.[26] The indirect exchange coupling constants govern the interaction of the conduction electrons and the local spins in the dots. They are given by

$$J_l=\frac{|W_l|^2}{\varepsilon_F-\varepsilon_l}, \quad J_r=\frac{|W_r|^2}{\varepsilon_l+Q-\varepsilon_F} \tag{66}$$

in case (b), and

$$J_l = |W_l|^2 \left(\frac{1}{\varepsilon_F - \varepsilon_l} + \frac{1}{\varepsilon_l + Q_l - \varepsilon_F} \right), \quad J_r = 0 \qquad (67)$$

in case (c). The last term H' in Eq. (64) includes irrelevant potential scattering terms arising in a second-order Schrieffer-Wolff transformation, and other invariants that appear in the Hausdorff expansion [Eq. (26)] i.e., mixed products like $\mathbf{S}_i \cdot [\mathbf{S}_j \times \mathbf{s}]$. These terms arise due to an interplay between the interdot exchange H_{lr} and the tunneling H_t. Here we do not consider these small corrections to the main Kondo effect.

Comparing Eq. (64) with Eq. (46), we see that the second-order terms of the expansion reproduce the general structure of a two-spin Hamiltonian. The interdot exchange has the same form for both representations, but there are significant differences in the values of the coupling constants between the leads and local spins. In particular, the tunnel coupling between the right dot and the leads is absent in this order in case (c), whereas in the two-spin representation [Eq. (43)] the coupling constants are $J_1 = (2 + \beta_2^2) J_l$ and $J_2 = \beta_2^2 J_l$. It should be noted, however, that a nonzero coupling between the leads and the right dot arises due to the interference between H_{lr} and $\mathcal{S}$ in a Schrieffer-Wolff representation, but its value differs from J_2. Thus, from the point of view of the general SO(4) symmetry of the DQD, the two-site representation is simply one more representation of the o_4 algebra as a direct sum of two o_3 algebras. The only case when the representations $\mathbf{S}_1, \mathbf{S}_2$ and $\mathbf{S}_l, \mathbf{S}_r$ coincide is in the symmetric DQD, where the admixture of excitons is ignored and the parity is conserved for an isolated DQD. This symmetric DQD, of course, also obeys an SO(4) symmetry, but its ground state is a singlet. The only way to activate the ''hidden symmetry'' in this case is to switch on a strong magnetic field that compensates for the exchange splitting. Then the effective spin Hamiltonian is given in Eq. (48), and a magnetic field-induced Kondo effect arises.

VI. CONCLUDING REMARKS

It is worth making several remarks about the advantages of using alternative approaches to analyze the physics of the quantum-spin rotator. We have presented three different ways of substituting spin-1/2 operators for the generic operators **S** and **P** of the SO(4) group. This substitution exposes numerous connections between the approach to the Kondo effect, treating the double dot as a spin rotator and the conventional description as a two-site Kondo problem. The traditional theory of the two-site Kondo effect[19] deals with a *symmetric* DQD, so it is formulated in terms of even-odd spin and charge states. The effects discussed in the present paper essentially arise only in *asymmetric* situations when $J_1 \gg J_2$ or $J_l \gg J_r$. In addition, we treated conduction electrons in a single-channel approximation, whereas the even-odd state classification of conduction electrons in a two-site Kondo model[28] classified it as a two-channel single-impurity model. Some generic properties of the two-spin Kondo effect are, nevertheless, similar in both limits. In particular, the competition between the on-site interactions $J_i(\mathbf{S}_i \cdot \mathbf{s})$ and the interdot exchange $J_{ij}(\mathbf{S}_i \cdot \mathbf{S}_j)$ results in the appearance of an unstable fixed point in the flow diagram dividing the Kondo singlet from an antiferromagnetic singlet ground states of the system. The conventional two-site Kondo impurity can also be classified as a ''spin rotator,'' and the singlet-triplet (even-odd) mixing is an essential part of the Kondo physics in this case.

Nano-objects whose symmetry is more complicated than localized spins, i.e., *quantum rotors* were discussed previously in a context of the theory of quantum phase transitions in two-dimensional Heisenberg antiferromagnets, spin ladders, and spin glasses (see, e.g., Ref. 29). A quantum rotor was defined as a spin whose rotation is constrained to move on a surface of an $(M \geqslant 2)$, dimensional sphere. An example of an array of quantum rotors is a double-layer system of antiferromagnetically ordered quantum spins. If the interlayer coupling $K_{12}(\mathbf{S}_{1m} \cdot \mathbf{S}_{2m})$ in a site m is stronger than the intersite coupling $J_{mn}(\mathbf{S}_{1m} \cdot \mathbf{S}_{1n})$ in a given layer, the pair of spins $\mathbf{S}_{1m}$ and $\mathbf{S}_{2m}$ form a quantum rotor $\mathcal{S}_m$ with an o_3 algebra and a Casimir operator $\mathcal{S}^2$. The spin rotator is a natural generalization of this description: in case of $M = 2$, the excited triplet state in each site m can be added to a manifold, and the ladder of spin rotors transforms into an array of spin rotators.

We leave a more detailed discussion of electron transport through DQD's for future communications, and briefly discuss a limiting case of a biased DQD with $J_r = 0$, which was realized experimentally.[11,12] In case (b), this limit corresponds to an electrometer geometry. In this configuration the right dot is isolated from the leads, but, nevertheless, it can be used for driving the current through the left dot. In Ref. 12 the driving was realized via an electrostatic coupling between the dots, and charge transfer was allowed this monitoring the Coulomb resonance conditions. In the present case, the resonance in a *spin* channel is allowed by modifying the energy of the *charge-transfer* exciton. To measure this effect one should choose an E window in a plan (V_g^r, V_g^l) for symmetric DQD's. At zero difference $V_g^r - V_g^l$, no Kondo effect should be observed. Then increasing this difference at given temperature T, one effectively changes the energy difference δ_0 [Eq. (25)] and raises the Kondo temperature T_K. When the regime $T \sim T_K$ is achieved, one finds oneself in a hatched region similar to that shown in Fig. 3(a) for a window {1,1}, and a zero-bias anomaly should appear in conductance.

In terms of the two-spin representation [Eq. (43)], the structure of the RG scheme remains the same, and the only change is a disappearance of the second term in Eq. (36) for J_T. The changes in the real-spin representation [Eq. (65)] are more essential, $J_r = 0$, and the Kondo tunneling occurs only through the left dot. However, the conventional theory of a single-site Kondo screening cannot be applied in this situation because the interdot tunneling term $\sim \overline{J_{lr}}$ is still present in Hamiltonian (64). If the renormalized coupling constant $\overline{J_{lr}}$ remains positive, the left spin is dynamically screened and the right spin remains free. This model is a limiting case of an underscreened spin-1 solution.

The description of the Kondo effect in terms of two fictitious spins **R** and **T** [Eqs. (49), and (50)] is another example

of separation of spin degrees of freedom into a dynamically confined moment **R** and an unscreened moment **T** (also see Ref. 6), and this case was realized in the experiments[4,5] mentioned above.

We have seen that the scaling trajectory for the coupling constant $\overline{\delta}=\overline{J_{lr}}$ is predetermined by the bare value of the singlet/triplet splitting $\delta_0=2\beta_1 V$, which, in turn, can be driven by the gate voltage [see Eq. (15)]. Thus we see that the Kondo tunneling channel in the left dot can be opened by softening the charge-transfer potential that is governed by the right gate voltage V_g^r, and a DQD with an isolated right dot works as a ''charge-spin transformer.''

The limit of zero J_r in case (c) was considered within the spin-rotator approach in Ref. 10. In terms of a full SO(4) description, the flow diagram is similar to that of a biased DQD [case (b)]. If one were to try to describe this asymmetric DQD in terms of screening of the individual spin $\mathbf{S}_l$, a problem would arise when taking into account charge fluctuations to the state $|Ex_l\rangle$ [Eq. (13)] at the first ''Haldane'' stage of the RG procedure, because this excitation is soft by assumption: $\omega_{ex,l}\ll D$. In this case the source of strong correlation is, in fact, the right dot, and the interdot tunneling is responsible for true spin-charge separation in the DQD. The description of Kondo tunneling in terms of the operators **S** and **P** is obviously preferable in this case.

In conclusion, here we considered the spin excitation spectrum and the Kondo effect in DQD's from the point of view of its generic symmetry, that is, an SO(4) symmetry of a quantum-spin rotator. The properties of spin rotators differ in many cases from those of localized spins with the same $\hat{S}^2$. In the case of a triplet ground state ($\hat{S}^2=2$), where cotunneling results in an underscreened Kondo effect, the presence of low-lying singlet excitation makes the Kondo temperature a nonuniversal quantity. If the ground state is a singlet ($\hat{S}^2=0$), the Kondo effect is nevertheless possible if one projection of the low-lying triplet excitation is involved in electron tunneling. An alternative language for discussing the properties of DQD's is provided by a two-site Kondo model approach. However, in spite of the overall SO(4) symmetry of the problem, an equivalence of these two approaches exists only in the case of conserved parity (symmetric DQD's). When the asymmetric charge-transfer exciton is admixed with a low-energy spin singlet, the two-site representation and the two-spin representation of the SO(4) group for a biased DQD are not equivalent.

ACKNOWLEDGMENTS

This work was partially supported by grants from the Israeli Science Foundations (Center of Excellence and Physics of complex quantum dots), a U.S.-Israel BSF grant (current instabilities in quantum dots), and the DIP program for quantum electronics in low-dimensional systems. We benefited from discussions with I. Krive, L.W. Molenkamp, and F. M. Peeters.

APPENDIX

The wave functions of symmetric and asymmetric DQD's occupied by one, two, or three electrons are listed below (also see Ref. 21). In addition, the tunnel matrix elements which connect the states from different charge sectors of the DQD's are presented. The eigenvalues and eigenfunctions of an isolated neutral DQD with $N=2$ can be found by direct diagonalization of Hamiltonians (4) and (5). In a neutral configuration $\{1,1\}$ the interdot capacitive coupling is absent. Far from Coulomb resonances when the inequalities (15) are valid, expansions (14) in symmetric case (a) and Eq. (13) in the asymmetric cases (b) and (c) give the following equations for the coefficients a_{ij} in first order of perturbation expansion in the tunnel coupling V. The processes taken into account in the mixing terms are shown by the dashed arrows in the upper panels of Fig. 1.

(a) Symmetric DQD:

$$a_{ee}=a_{ss}\approx 1-\beta^2, \quad a_{se}=-a_{es}=\sqrt{2}\beta. \tag{A1}$$

(b) Biased DQD:

$$\begin{aligned} a_{ss}&=1-\beta_1^2-\beta_1'^2, \quad a_{sl}=-a_{ls}=\sqrt{2}\beta_1', \\ a_{sr}&=-a_{rs}=\sqrt{2}\beta_1, \\ a_{ll}&=1-\beta_1'^2, \quad a_{rr}=1-\beta_1^2. \end{aligned} \tag{A2}$$

Here $\beta_1'=V/(Q+\Delta)$. We assume that $\beta_1'\ll\beta_1$ and neglect the terms $\sim\beta_1'$ in our calculations.

(c) Asymmetric DQD:

$$\begin{aligned} a_{ss}&=1-\beta_2^2-\beta_2'^2, \quad a_{sl}=-a_{ls}=\sqrt{2}\beta_2, \\ a_{sr}&=-a_{rs}=\sqrt{2}\beta_2', \\ a_{ll}&=1-\beta_2^2, \quad a_{rr}=1-\beta_2'^2. \end{aligned} \tag{A3}$$

Here $\beta_2'=V/(Q_r-\Delta)\ll\beta_2$, and we neglect the corresponding contributions as well.

To complete the enumeration of states involved in the tunneling Hamiltonian [Eq. (1)], one should define the charge states of DQD's which arise in a process of electron tunneling between DQD's and metallic leads. We are interested in one-electron tunneling, so the states with one and three electrons in DQD's, $N=1$ and 3, should be taken into account.

(a) *Symmetric DQD's.* One-electron states are even and odd combinations of electronic wave functions belonging to the left and right wells. The same is valid for the three-electron states, which in fact are the hole analogs of one-electron states:

$$\begin{aligned} |1e,\sigma\rangle&=\frac{1}{\sqrt{2}}(d_{l\sigma}^\dagger+d_{r\sigma}^\dagger)|0\rangle, \\ |1o,\sigma\rangle&=\frac{1}{\sqrt{2}}(d_{l\sigma}^\dagger-d_{r\sigma}^\dagger)|0\rangle, \\ |3e,\sigma\rangle&=\frac{1}{\sqrt{2}}(d_{l\sigma}^\dagger d_{r\downarrow}^\dagger d_{r\uparrow}^\dagger+d_{r\sigma}^\dagger d_{l\downarrow}^\dagger d_{l\uparrow}^\dagger)|0\rangle, \end{aligned} \tag{A4}$$

$$|3o,\sigma\rangle=\frac{1}{\sqrt{2}}(d^\dagger_{l\sigma}d^\dagger_{r\downarrow}d^\dagger_{r\uparrow}-d^\dagger_{r\sigma}d^\dagger_{l\downarrow}d^\dagger_{l\uparrow})|0\rangle.$$

(b) and (c) Asymmetric DQD's. In this case the DQD is ''polarized'' both in negatively and positively charged states. The one-electron wave functions are the same in cases (b) and (c):

$$|1a,\sigma\rangle=(\sqrt{1-\alpha^2}d^\dagger_{l\sigma}-\alpha d^\dagger_{r\sigma})|0\rangle,$$

$$|1b,\sigma\rangle=(\alpha d^\dagger_{l\sigma}+\sqrt{1-\alpha^2}d^\dagger_{r\sigma})|0\rangle \quad \text{(A5)}$$

$(\alpha=V/\Delta)$. The corresponding energy levels are

$$E_{1a}=\varepsilon_l+\alpha V, \quad E_{1b}=\varepsilon_r-\alpha V. \quad \text{(A6)}$$

The three-electron wave functions are represented by expressions

$$|3b,\sigma\rangle=(\sqrt{1-\alpha^2}d^\dagger_{l\sigma}d^\dagger_{r\downarrow}d^\dagger_{r\uparrow}+\alpha d^\dagger_{r\sigma}d^\dagger_{l\downarrow}d^\dagger_{l\uparrow})|0\rangle,$$

$$|3a,\sigma\rangle=(-\alpha d^\dagger_{l\sigma}d^\dagger_{r\downarrow}d^\dagger_{r\uparrow}+\sqrt{1-\alpha^2}d^\dagger_{r\sigma}d^\dagger_{l\downarrow}d^\dagger_{l\uparrow})|0\rangle \quad \text{(A7)}$$

in case (b), and

$$|3b,\sigma\rangle=(\sqrt{1-\alpha'^2}d^\dagger_{r\sigma}d^\dagger_{l\downarrow}d^\dagger_{l\uparrow}+\alpha' d^\dagger_{l\sigma}d^\dagger_{r\downarrow}d^\dagger_{r\uparrow})|0\rangle,$$

$$|3a,\sigma\rangle=(-\alpha' d^\dagger_{r\sigma}d^\dagger_{l\downarrow}d^\dagger_{l\uparrow}+\sqrt{1-\alpha'^2}d^\dagger_{l\sigma}d^\dagger_{r\downarrow}d^\dagger_{r\uparrow})|0\rangle \quad \text{(A8)}$$

in case (c). Here $\alpha'=V/(Q_r-Q_l-\Delta)$. The eigenlevels are given by the equations

$$E_{3b}=2\varepsilon_r+Q-\alpha V, \quad E_{3a}=2\varepsilon_l+Q+\alpha V \quad \text{(A9)}$$

in case (b) and

$$E_{3b}=2\varepsilon_l+Q_l-\alpha' V, \quad E_{3a}=2\varepsilon_r+Q_r+\alpha' V \quad \text{(A10)}$$

in case (c).

The tunneling matrix elements in Hamiltonian H_t [Eq. (11)] include states from different charge sectors $N(\nu_l,\nu_r)$ of the dot Hamiltonian H_d [Eq. (9)]. In the presence of an interdot coupling V, and at nonzero bias potential $V_g^l-V_g^r>0$, the numbers ν_l and ν_r are nonintegers, and the tunneling transparencies of the left and right dots are different even if $W_l=W_r$ [case (b)]. In case (c), the tunneling barrier between the leads and the right dot is wider, and one can assume that $W_r<W_l$, so that the asymmetry is even stronger. Considering the asymmetric configurations in case (b), we note that the expansion coefficients in Eq. (13) for the two-electron states $|\Lambda\rangle$ are such that $a_{ss}\gg a_{sl},a_{sr}$ [see Eq. (A2)]. The tunnel matrix elements which define the dominant contributions to the RG equations (20) are

$$W^{TO,1\bar{\sigma}}_{qu\sigma}=\frac{1}{\sqrt{2}}w_l,$$

$$W^{T\pm,1\pm}_{qu\pm}=w_l, \quad W^{TO,3\bar{\sigma}}_{qd\sigma}=\frac{\sigma}{\sqrt{2}}w_r,$$

$$W^{T\pm,3\pm}_{qd\pm}=\sigma w_r, \quad \text{(A11)}$$

$$W^{S,1\bar{\sigma}}_{qu\sigma}=\frac{1}{\sqrt{2}}\sigma a_{ss}w_l,$$

$$W^{S,3\bar{\sigma}}_{qd\sigma}=\frac{1}{\sqrt{2}}a_{ss}w_r,$$

(here $w_l=\sqrt{1-\alpha^2}W_l$). Similar equations can be derived in case (c), where the wave functions of the virtual charged states $|1b\sigma\rangle$ and $|3b\sigma\rangle$ are given by Eqs. (A5) and (A8). Now, instead of Eq. (A11), one has

$$W^{TO,1\bar{\sigma}}_{qu\sigma}=\frac{1}{\sqrt{2}}w_l, \quad W^{T\pm,1\pm}_{qu\pm}=w_l,$$

$$W^{TO,3\bar{\sigma}}_{qd\sigma}=\frac{\sigma}{\sqrt{2}}w'_l, \quad W^{T\pm,3\pm}_{qd\pm}=\sigma w_r, \quad \text{(A12)}$$

$$W^{S,1\bar{\sigma}}_{qu\sigma}=\frac{1}{\sqrt{2}}\sigma a_{ss}w_l, \quad W^{S,3\bar{\sigma}}_{qd\sigma}=\frac{1}{\sqrt{2}}a_{ss}w'_l,$$

where $w'_l=\sqrt{1-\alpha'^2}w_l$.

[1] *Mesoscopic Electron Transport*, edited by L. L. Sohn, L. P. Kouwenhoven, and G. Schön (Kluwer, Dordrecht, 1997).

[2] D. Goldhaber-Gordon *et al.*, Phys. Rev. Lett. **81**, 5225 (1998); S.M. Cronenwett *et al.*, Science **281**, 540 (1998); F. Simmel *et al.*, Phys. Rev. Lett. **83**, 804 (1999).

[3] M. Pustilnik, Y. Avishai, and K. Kikoin, Phys. Rev. Lett. **84**, 1756 (2000).

[4] J. Nygård, D.H. Cobden, and P.E. Lindelof, Nature (London) **408**, 342 (2000).

[5] N.S. Sasaki *et al.*, Nature (London) **405**, 764 (2000).

[6] D. Giuliano and A. Tagliacozzo, Phys. Rev. Lett. **84**, 4677 (2000); D. Giuliano, B. Jouault, and A. Tagliacozzo, Phys. Rev. B **63**, 125318 (2001).

[7] M. Eto and Yu.V. Nazarov, Phys. Rev. Lett. **85**, 1306 (2000); Phys. Rev. B **64**, 085322 (2001).

[8] M. Pustilnik and L. Glazman, Phys. Rev. Lett. **85**, 2993 (2000); Phys. Rev. B **64**, 045328 (2001).

[9] L.I. Glazman and M.E. Raikh, Pis'ma Zh. Éksp. Teor. Fiz. **67**, 1276 (1988) [JETP Lett. **47**, 452 (1988)]; T.K. Ng and P.A. Lee, Phys. Rev. Lett. **61**, 1768 (1988).

[10] K. Kikoin and Y. Avishai, Phys. Rev. Lett. **86**, 2090 (2001).

[11] F. Hofmann, T. Heinzel, D.A. Wharam, J.P. Kotthaus, G. Böm, W. Klein, G. Tränkle, and G. Weimann, Phys. Rev. B **51**, 13 872 (1995).

[12] L.W. Molenkamp, K. Flensberg, and M. Kemerlink, Phys. Rev. Lett. **75**, 4282 (1995).

[13] U. Wilhelm and J. Weis, Physica E **6**, 668 (2000); T. Pohjola, H. Schöller, and G. Schön, Europhys. Lett. **54**, 241 (2001).

[14] K. Flensberg, A. A. Odintsov, F. Liefrink, and P. Teunissen, Int. J. Mod. Phys. **B13**, 21-22, 2651 (1999).

[15] The coupled vertical dots are objects where these effects are investigated in many details. See, e.g., S. Tarucha, J. Phys. Condens. Matter **11**, 60213 (1999); M. Rontani, F. Rossi, F. Manghi, and E. Molinari, Solid State Commun. **112**, 151 (1999); B. Partoens and F.M. Peeters, Phys. Rev. Lett. **84**, 4433 (2000).

[16] A. Georges and Y. Meir, Phys. Rev. Lett. **82**, 3508 (1999).

[17] Pairs of dots of essentially different radii and capacitances placed in series were studied by R.H. Blick, R.J. Haug, J. Weis, D. Pfannkuche, K.v. Klitzing, and K. Eberl, Phys. Rev. B **53**, 7899 (1996). In this case the ration of capacitive energies of two dots was as large as $Q_l/Q_r \approx 4$.

[18] R. Ugajin, Int. J. Mod. Phys. **13**, 2689 (1999).

[19] B.A. Jones and C.M. Varma, Phys. Rev. Lett. **58**, 843 (1987); B.A. Jones, C.M. Varma, and J.W. Wilkins, *ibid.* **61**, 125 (1988); B.A. Jones and C.M. Varma, Phys. Rev. B **40**, 324 (1989); I. Affleck, A.W.W. Ludwig, and B.A. Jones, *ibid.* **52**, 9528 (1995); J.B. Silva *et al.*, Phys. Rev. Lett. **76**, 275 (1996).

[20] In the general case of a noninteger $\nu_{l,r}$ the interdot Coulomb and exchange interactions arise because of the charge transfer in asymmetric configurations (b) and (c). This interaction is $\sim \beta_j^4$ ($j=1$ and 2, respectively), and we neglect it in further calculations.

[21] The same type of strongly correlated two-site states appear in the cluster approach to the Hubbard and Anderson lattice models: W.N. Mei and Y.C. Lee, Phys. Rev. B **24**, 1111 (1981); A.V. Vedyaev, M.E. Zhuravlev, V.A. Ivanov, and M. Marinaro, Theor. Math. Phys. **108**, 930 (1996).

[22] F.D.M. Haldane, Phys. Rev. Lett. **40**, 416 (1978).

[23] P.W. Anderson, J. Phys. C **3**, 2436 (1970).

[24] J.R. Schrieffer and P.A. Wolff, Phys. Rev. **149**, 491 (1966).

[25] M. J. Englefield, *Group Theory and the Coulomb Problem* (Wiley, New York, 1972).

[26] A.B. Harris and R.V. Lange, Phys. Rev. **157**, 259 (1967).

[27] Ph. Nozieres and A. Blandin, J. Phys. (Paris) **41**, 193 (1980).

[28] A. Moustakas and D. Fisher, Phys. Rev. B **51**, 6908 (1995).

[29] S. Sachdev, *Quantum Phase Transitions* (Cambridge University Press, Cambridge, 1999), Chap. 5.